

Effects of Multiple Strengthening Treatments on Mechanical Properties and Stability of Nanoscale Precipitated Phases in an Aluminum-Copper-Lithium Alloy

S. Ahmadi^{1)†}, H. Arabi²⁾ and A. Shokuhfar³⁾

1) Department of Material Science, Faculty of Engineering, Tarbiat Modares University, Tehran, Iran

2) Center of Excellence of Advanced Materials and Processing (CEAMP), Department of Metallurgy and Materials Science and Engineering, Iran University of Science & Technology (IUST), Narmak, Tehran, Iran

3) Department of Material Science, Faculty of Mechanical Engineering, K.N. Toosi University of Technology, Tehran, Iran

[Manuscript received May 21, 2009, in revised form January 28, 2010]

Effects of multiple strengthening treatments (*i.e.* aging either at three or four consecutive temperatures) on mechanical properties and stability of nanoscale precipitated phases in an AA2090 alloy have been evaluated in this research. Various tests such as hardness, tensile, electrical resistance, differential scanning calorimetric (DSC), and transmission electron microscopy (TEM) have been performed. The results show that the ultimate tensile strength (UTS) and the yield strength of the samples aged at four consecutive temperatures (*i.e.* natural aging+190°C+150°C+100°C) can be increased approximately to 660 and 610 MPa, respectively. It is also found that precipitation of T1 phase occurs during multiple aging process of the alloy and the higher amounts of enthalpies shown in DSC charts are linked to higher volume fraction of this precipitate. Furthermore, TEM observations reveal that T1 phase has plate shape morphology and its crystal structure is in the form of hcp with lattice parameters of $a=0.467$ nm and $c=0.878$ nm.

KEY WORDS: Multiple strengthening; Thermo mechanical treatment (TMT); Selected area electron diffraction (SAED) pattern; Inter planar spacing (d)

1. Introduction

Reducing weight and improvement of the E/ρ ratio (*i.e.* E : elastic modulus and ρ : density) in metallic materials used in many industries are mentioned as the most important approaches toward the application of Al-Li alloys as demonstrated by Rioja^[1] and Starink *et al.*^[2]. Indeed, it is found that density of aluminum alloys can be reduced approximately 3% by addition of 1% lithium while their elastic modulus can be improved up to 6%^[1,3]. In other words, the physical and mechanical properties of aluminum alloys may be dramatically changed by addition of lithium. In this case, changes may be due to consid-

erable decrease in density (up to 10%) and drastic increase in elastic modulus (up to 15%) as shown by Fridlyander^[3] and Kim *et al.*^[4].

Thermo mechanical treatments (TMT) for improvement of mechanical properties of Al-Li alloys are widely used in order to ease the production of the alloy in industry. It is true that a wide variety of strengthening phases, such as T₁ (Al₂CuLi), δ' (Al₃Li), and T₂ (Al₂Li₃Cu) are precipitated within the microstructures of these types of alloys during TMT, determining their physical and mechanical properties. In particular, T₁ phase is known as one of the most effective strengthening phases in Al-Cu-Li alloys as shown by Ahmadi *et al.*^[5,6].

In term of TMT processes, aging treatment in consecutive temperatures (*i.e.* multiple strengthening treatments) can be used to achieve exotic mechani-

† Corresponding author. Ph.D.; Tel.: +98 261 3505096; E-mail address: Ahmadi.amrc@gmail.com (S. Ahmadi).

cal properties in AA8090 alloy. It is worth mentioning that, “multiple strengthening processes” is a term which refers to a sequence of heat treatments of an alloy in two, three, four or more different temperatures. In fact, formation of strengthening precipitates and their stabilization in each cycle of aging treatment is main objective of multiple strengthening processes. Although application of these processes are wide open for Al-Li alloys, only a few researches have involved themselves in this matter as it has been mentioned by Xia^[7] and Gable *et al.*^[8].

In practice, double stage aging process with subsequent cold working (after solution annealing process) was effectively used to enhance the tensile properties of the Al-Li alloys; in this field, the research by Fridlyander *et al.*^[9] on the effects of two-stage aging treatment on properties of 1441 alloy is a good example. Furthermore, increasing hardness and tensile strength of an Al-Li sheet alloy *via* precipitation of steady state phases in the first step of aging process is another excellent example^[10]. In addition to the improvement of hardness and tensile strength of Al-Li alloys, enhancement of other mechanical and physical properties by multi step aging process has been reported by some other researchers^[11–13].

The effects of application of either three or four cycles of aging on some properties of an AA2090 alloy were evaluated for the first time in this research. Furthermore, precipitation and characteristics of T₁ phase in the alloy were studied by differential scanning calorimetric (DSC) and transmission electron microscopy (TEM).

2. Experimental

A hot rolled sheet of Al-Cu-Li-Zr (AA2090) alloy with a thickness of 2.7 mm and chemical composition shown in Table 1 was utilized for this investigation.

Table 1 Chemical composition of the alloy (wt pct)

Cu	Li	Zr	Fe, Si	Al
3.1	2.2	0.12	<0.3	Bal.

After solution treatment at 535°C for 90 min, the samples were quenched in ice-water and then cold rolled (C.R.) (10% reduction in thickness). Later, the specimens were aged at 190 and 150°C in three and four different cycles according to relations (1) to (5) below (N.A. means natural aging).

$$\text{N.A. (45 d) + 150}^\circ\text{C/6 - 100 h} \quad (1)$$

$$\text{N.A. (45 d) + 190}^\circ\text{C/1 - 48 h} \quad (2)$$

$$\text{N.A. (45 d) + 150}^\circ\text{C/48 h + 190}^\circ\text{C/6 h} \quad (3)$$

$$\text{N.A. (45 d) + 150}^\circ\text{C/48 h + 190}^\circ\text{C/6 h + 100}^\circ\text{C/100 h} \quad (4)$$

$$\text{N.A. (45 d) + 190}^\circ\text{C/6 h + 150}^\circ\text{C/48 h + 100}^\circ\text{C/100 h} \quad (5)$$

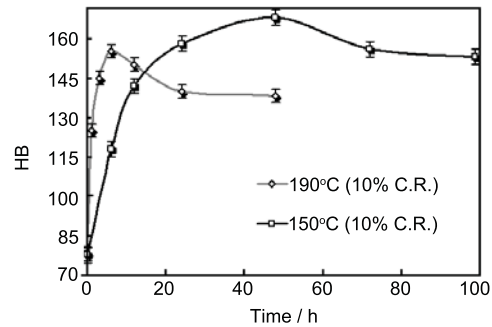


Fig. 1 Hardness *vs* aging time under two different aging conditions

A Koopa (UV1) hardness tester was used to determine the hardness of the samples according to ASTM E45 standard. Specimens were also subjected to tensile test according to ASTM E8 standard. Electrical resistance was measured by using a micro-ohmmeter having 1 $\mu\Omega$ accuracy.

In addition, calorimetric test was carried out with a DSC tester (NEC-409pc) over the temperature range of 50–550°C at heating rate of 10°C/min. Argon gas was used as both purge and protective gas during DSC tests. In practice, base line in DSC tests was determined by “empty pan” method.

Moreover, evaluation of phase’s characteristics was accomplished by using a Philips CM200 transmission electron microscope (200 KV). The specimens were polished by 25% nitric acid and 75% methanol solvent in a twin jet polisher before examining them under TEM.

3. Results and Discussion

3.1 Hardness test

Before precipitation hardening treatments at 150 and 190°C, all the specimens were subjected to natural aging in air for 45 d. Variation of hardness at 150 and 190°C *vs* aging time is shown in Fig. 1. This figure shows that hardness increases gradually with aging time and comes to its peak at 48 and 6 h for the samples aged at 150 and 190°C, respectively. Thus, these aging conditions (*i.e.* 150°C/48 h and 190°C/6 h) were chosen as the base for three steps aging process for each case.

In effect, three sets of aging processes were performed at two different temperatures according to aging conditions (3) to (5).

In Fig. 2, variation of hardness for samples aged according to multiple strengthening treatments is shown. As can be observed in this figure, the hardness of the specimens heat-treated at three and four aging consecutive temperatures is definitely higher than those of the other specimens.

3.2 Mechanical and electrical resistance tests

Yield strength and ultimate tensile strength

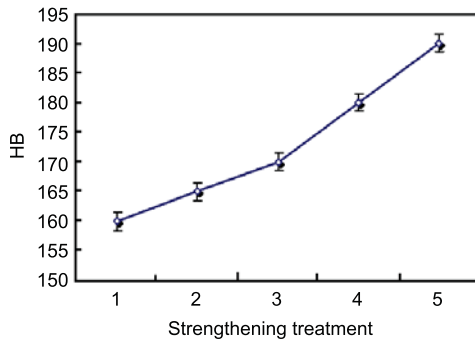


Fig. 2 Effect of heat treatment conditions on variation of hardness. 1—N.A. (45 d)+190°C/6 h, 2—N.A. (45 d)+150°C/48 h, 3—N.A. (45 d)+150°C/48 h+190°C/6 h, 4—N.A. (45 d)+150°C/48 h+190°C/6 h+100°C/100 h, 5—N.A. (45 d)+190°C/6 h+150°C/48 h+100°C/100 h

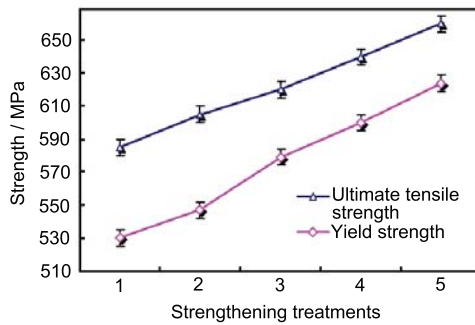


Fig. 3 Effect of heat treatment conditions on variation of UTS and yield strength. 1—N.A. (45 d)+190°C/6 h, 2—N.A. (45 d)+150°C/48 h, 3—N.A. (45 d)+150°C/48 h+190°C/6 h, 4—N.A. (45 d)+150°C/48 h+190°C/6 h+100°C/100 h, 5—N.A. (45 d)+190°C/6 h+150°C/48 h+100°C/100 h

(UTS) of the aged samples are shown in Fig. 3. It is clear that both of yield strength and UTS gradually rise as the heat treatment conditions change from (1) to (5), so that the UTS and yield strength of the sample aged according to condition (5) increase to about 660 and 610 MPa, respectively. This advance in the strength of the alloy can be related to the formation of stable strengthening precipitates and phases in the structure. It is known that electrical resistance in heat treatable alloys (*e.g.* Al-Li) can be drastically influenced by precipitation reactions^[6].

Electrical resistance data are very useful for studying the initial stages of aging process and provide indirect evidence on the relation between the available solute atoms and formation of the precipitates. In fact, effects of solute atoms on electron scattering are more important than those of grain boundaries, dislocation, and precipitates according to Riontino and Abis^[14] and Gao *et al.*^[15]. In other words, solute atoms, clusters and GP zones disrupt electron flow through the lattice and decrease the conductivity of

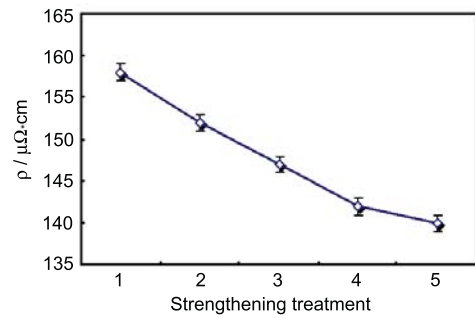


Fig. 4 Relationship between electrical resistance and aging treatments. 1—N.A. (45 d)+190°C/6 h, 2—N.A. (45 d)+150°C/48 h, 3—N.A. (45 d)+150°C/48 h+190°C/6 h, 4—N.A. (45 d)+150°C/48 h+190°C/6 h+100°C/100 h, 5—N.A. (45 d)+190°C/6 h+150°C/48 h+100°C/100 h

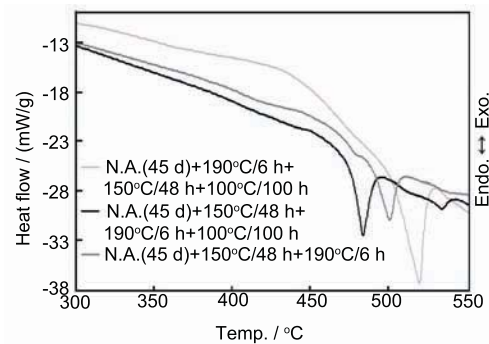


Fig. 5 DSC curves of the specimens aged in three different aging methods

the alloy effectively.

Figure 4 demonstrates the electrical resistance of aged specimens for various aging methods. It is indicated that the electrical resistance of the samples declines after aging treatments of alloy in three and four consecutive temperatures. This effect seems to be due to the formation of precipitates in the microstructure of the alloy during its aging.

It should be noted that the data presented in Figs. 3 and 4 are compatible; minimum of the electrical resistance and maximum of strength both belong to the sample aged according to condition (5). Consequently, the mechanical properties of the alloy can be effectively increased during aging treatment in multiple cycles due to the formation of strengthening phases in its microstructure.

3.3 DSC test

It is known that DSC can be effectively used to determine type and stability of phases in structure of the alloys. Three samples were heat treated according to conditions (3) to (5) and then subjected to DSC test at a heating rate of 10°C/min. Endothermic and exothermic peaks due to the formation and dissolution of phases in the aged specimens are shown in Fig. 5.

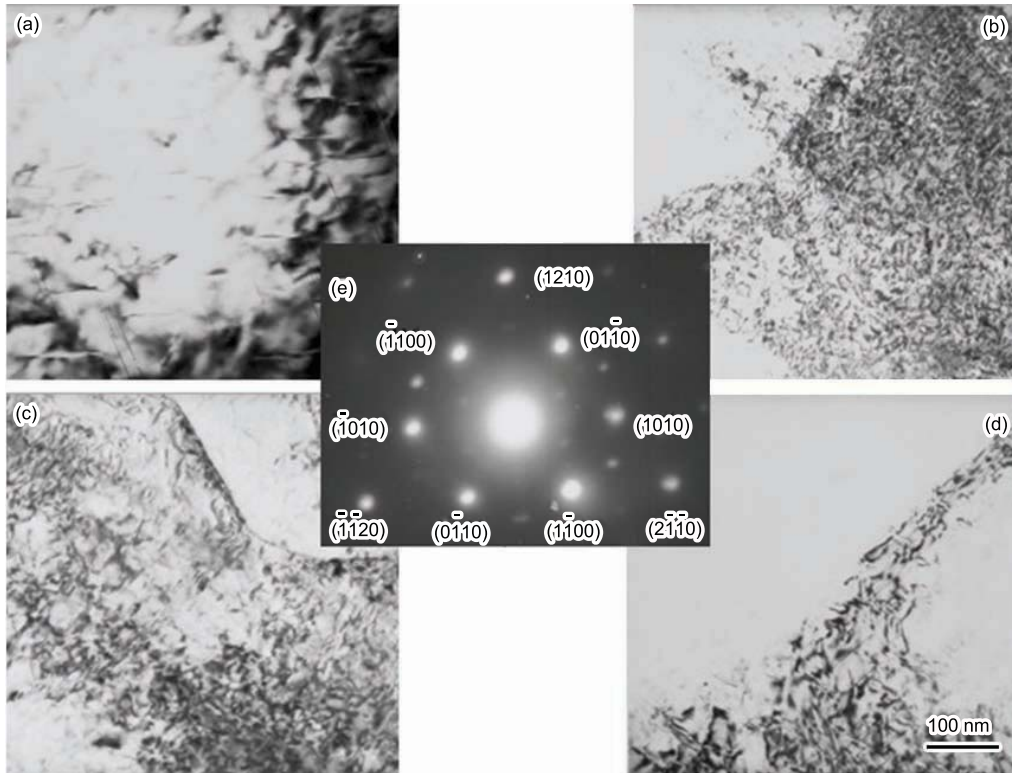


Fig. 6 Microstructure of the alloy heat treated according to condition: N.A. (45 d)+190°C/6 h+150°C/48 h+100°C/100 h aging method. (a) and (b) microstructure of the alloy showing plate-shaped morphology of T_1 phase, (c) image showing precipitation of T_1 phase in the grains, (d) image showing precipitation of T_1 phase near the grain boundaries in the structure of the alloy, (e) SAED pattern of T_1 phase which is completely compatible with hcp lattice

Figure 5 shows that there are three successive endothermic peaks which can be attributed to dissolution of some phases. It is also clear that these endothermic effects appear approximately between 480 and 520°C in DSC curves. These effects are definite indications toward the dissolution of phases such as T_1 , T_2 and T_B in the microstructure. According to the research by Davydov *et al.*^[16], temperature range for dissolution of T_1 phase in the DSC curves is 440–510°C. Therefore, T_1 phase precipitated in the microstructure of the alloy due to multiple strengthening treatments in regard to the result of DSC tests.

One of the most striking features observed in Fig. 5 is the extent of heat flow in each peak. As a matter of fact, sample aged according to condition (5) differs from the other specimens, probably because of its extended dissolution effect caused by high volume fraction of phases. In principle, volume fraction of precipitates in the microstructures of heat treatable alloys can be linked to enthalpy of dissolution, ΔH^d , in calorimetric diagrams such as the one presented by Yan and Starink^[17]. With respect to Fig. 5, heating rate (10°C/min) and Eq. (6) below, ΔH^d can be calculated (Table 2).

$$C_p = \frac{d(\Delta H)}{dT} \quad (6)$$

Table 2 Calculated enthalpy of heat-treated specimens according to previous conditions (1)–(5) and Eq. (6)

Strengthening treatment	ΔH^d /(mJ/g)
3	–5.4
4	–8
5	–9.1

Indeed, T_1 phase was formed in all specimens (aged in one or more steps) and the bigger dissolution effects (enthalpy) in DSC diagram were caused by the higher volume fraction of phases or precipitates in the microstructure. In other words, in both multiple strengthening treatments and general aging heat treatments, T_1 phase was formed in the structure; but in cyclic aging process (*e.g.* according to Eq. (4)), volume fraction of the phase was higher than those of the other. With regard to DSC test results, therefore, volume fraction of strengthening phases can be effectively increased during multiple strengthening treatments.

3.4 TEM observation

Even though it is believed that there are some kinds of strengthening phases in the structure of Al-Cu-Li (*e.g.* AA2090 and AA8090) alloys (*i.e.* T_1 ,

T₂, T_B), only T₁ (Al₂CuLi) phase has been normally named as pre-eminent phase responsible for enhancing hardness and strength of Al-Cu-Li alloys, especially in AA2090 alloy as reported by Chen and Bhat^[18] and Liu *et al.*^[19].

This nanoscale hexagonal closed-packed phase has a plate-shaped morphology^[18]. Typical microstructure of the alloy and selected area electron diffraction (SAED) pattern of the precipitated phases are shown in Fig. 6. It shows that morphology of strengthening phase is in the form of plate. Moreover, the SAED pattern of the alloy prepared according to condition (5) is completely compatible with hcp lattice.

The lattice parameters of the hexagonal precipitate T₁ (*i.e.* a and c) were calculated by considering the camera constant (λL) and inter-planar spacing (d). In principle, a and c were calculated in this research as 0.467 and 0.878 nm, respectively. In some other researches by Yoshimura *et al.*^[20], the amounts of lattice parameters reported are a bit different from those we obtained in this research; *e.g.* $a=0.496$ nm and $c=0.935$ nm were reported for T₁ precipitate. This difference seems to be caused by the fact that the chemical composition of alloy and the type of heat treatment can slightly change the lattice parameters.

DSC evaluations and TEM observations showed that nano size T₁ (Al₂CuLi) phase precipitated in the structure of the Al-Cu-Li alloy due to the multiple strengthening aging treatment.

4. Conclusions

(1) UTS and hardness can be increased effectively up to 660 MPa and 190 HB, respectively in AA2090 alloy by applying multiple strengthening treatments.

(2) Endothermic effects in DSC diagrams of AA2090 alloy occur between 480 and 520°C and can be attributed to the dissolution of T₁ phase.

(3) Higher amount of enthalpy (bigger dissolution effects in DSC diagram) are linked to the higher volume fraction of phases or precipitates in the structure of the alloy aged in quadruple strengthening treatment.

(4) Plate-shaped morphology and hcp lattice was the most striking feature of the nanoscale strengthening precipitate (*i.e.* T₁) according to TEM observations. This phase was also observed in the structure of

the alloy aged in quadruple strengthening treatment.

(5) Lattice parameters a and c of the hcp structure of T₁ phase were measured as 0.467 and 0.878 nm, respectively.

REFERENCES

- [1] R.J. Rioja: *Mater. Sci. Eng. A*, 1998, **257**, 100.
- [2] M.J. Starink, A. Cerezo, J.L. Yan and N. Gao: *Philos. Mag. Lett.*, 2006, **86**, 243.
- [3] I.N. Fridlyander: *Mater. Sci. Forum*, 2000, **331-337**, 921.
- [4] J.M. Kim, K.D. Seong, J.H. Jun, K. Shin, K.T. Kim and W.J. Jung: *J. Alloy. Compd.*, 2007, **434-435**, 324.
- [5] S. Ahmadi and A. Shokuhfar: *Def. Diff. Forum*, 2008, **273-276**, 14.
- [6] S. Ahmadi, H. Arabi and A. Shokuhfar: *J. Alloy. Compd.*, 2009, **484**, 90.
- [7] X.X. Xia: *Scripta Metall. Mater.*, 1992, **26**(10), 1587.
- [8] B.M. Gable, A.A. Csontos and E.A. Starke Jr.: *J. Light Met.*, 2002, **2**, 65.
- [9] J.N. Fridlyander, V.V. Antipov and T.P. Fedorenko: *Mater. Forum*, 2004, **28**, 1051.
- [10] S. Ahmadi and A. Shokuhfar: *Def. Diff. Forum*, 2008, **273-276**, 18.
- [11] J. Mizera and K.J. Kurzydowski: *Scripta Mater.*, 2001, **45**, 801.
- [12] R.K. Bird, D.L. Dicus, J.N. Fridlyander and V.S. Sandler: *Mater. Sci. Forum*, 2000, **331-337**, 907.
- [13] A. Dupasquier, A. Somoza, R.N. Lumley and I.J. Polmear: *Mater. Forum*, 2004, **28**, 1135.
- [14] G. Riontino and S. Abis: *Mater. Sci. Forum*, 2002, **396-402**, 771.
- [15] N. Gao, M.J. Starink, L. Davin, A. Cerezo, S.C. Wang and P.J. Gregson: *Mater. Sci. Technol.*, 2005, **21**, 1010.
- [16] V.G. Davydov, J.N. Fridlyander, M.V. Samarina, A.I. Orozov, L.B. Ber, V.I. Yelagin, R. Lang and T. Pfannenmuller: *Mater. Sci. Forum*, 2000, **331-337**, 1049.
- [17] J.L. Yan and M.J. Starink: *Modelling of Precipitation and Yield Strength in Al-Cu-Mg Alloys*, in Proc. 13th National Symp. on *Phase Diagrams*, Xiamen, China, 2006, 658.
- [18] P.S. Chen and B.N. Bhat: *NASA/TM-200-211548*, Alabama, 2002.
- [19] T. Liu, Q. Wang, H. Zhang, K. Wang, X. Pang and J. He: *J. Alloy. Compd.*, 2009, **469**, 258.
- [20] R. Yoshimura, T. Konno, E. Abe and K. Hiraga: *Acta Mater.*, 2003, **51**, 4251.